Published in final edited form as:
Science. 2008 August 15; 321(5891): 970–974. doi:10.1126/science.1159194.

In vivo imaging reveals an essential role for neutrophils in Leishmaniasis transmitted by sand flies

Nathan C. Peters[1,2], **Jackson G. Egen**[1,3], **Nagila Secundino**[2], **Alain Debrabant**[4], **Nicola Kimblin**[2], **Shaden Kamhawi**[2], **Phillip Lawyer**[2], **Michael P. Fay**[5], **Ronald N. Germain**[3,6], and **David Sacks**[2,6]

[2]Laboratory of Parasitic Diseases, National Institute of Allergy and Infectious Diseases, National Institutes of Health, Bethesda, MD, 20892, USA.

[3]Laboratory of Immunology, National Institute of Allergy and Infectious Diseases, National Institutes of Health, Bethesda, MD, 20892, USA.

[4]Division of Emerging and Transfusion Transmitted Diseases, OBRR, CBER, Food and Drug Administration, Bethesda, MD 20892, USA.

[5]Biostatistics Research Branch, National Institute of Allergy and Infectious Diseases, National Institutes of Health, Bethesda, MD, 20892, USA.

Abstract

Infection with the obligate intracellular protozoan *Leishmania* is thought to be initiated by direct parasitization of macrophages, but the early events following transmission to the skin by vector sand flies have been difficult to examine directly. Using dynamic intravital microscopy and flow cytometry, we observed a rapid and sustained neutrophilic infiltrate at localized sand fly bite sites. Invading neutrophils efficiently captured *Leishmania major* (*L.m.*) parasites early after sand fly transmission or needle inoculation, but phagocytosed *L.m.* remained viable and infected neutrophils efficiently initiated infection. Furthermore, neutrophil depletion reduced, rather than enhanced, the ability of parasites to establish productive infections. Thus, *L.m.* appears to have evolved to both evade and exploit the innate host response to sand fly bite in order to establish and promote disease.

Many parasitic diseases are transmitted by the bite of an infected arthropod, yet the dynamics of the host-parasite interaction in this context remain largely uncharacterized. Transmission of *Leishmania* by infected sand fly bite represents an attractive experimental system to study early inflammatory responses and relate these processes to the establishment of an infectious disease. Leishmaniasis is thought to be initiated by direct parasitization of macrophages following deposition into the skin (1). However, the ability of neutrophils to rapidly respond to and efficiently phagocytose a variety of pathogens suggests they may also be an initial target of *Leishmania* infection (2–4). Indeed, following needle injection of *L.m.*, infected neutrophils have been observed, and both host protective and disease promoting roles for these cells have been reported (5–10). Importantly, the role of neutrophils has never been addressed in sand fly-transmitted *Leishmania* infections.

Sand fly biting involves wounding of the microvasculature to create a hemorrhagic pool from which to feed, a process that initiates a strong local inflammatory response (11–13). In

Correspondence regarding sand flies and *Leishmania* infection should be addressed to D.L.S., (dsacks@nih.gov). Correspondence regarding intravital imaging should be addressed to J.G.E., (jegen@niaid.nih.gov).
[1,6]These authors contributed equally to this work.

order to further characterize the host response at the site of sand fly bite, uninfected or *L.m.*-infected *Phlebotomus duboscqi* sand flies, a natural vector of *L.m.*, were allowed to feed on the ears of C57BL/6 mice (14,15) which develop self-healing cutaneous lesions similar to the human disease. Flow cytometric analysis revealed a dramatic and sustained infiltration of neutrophils into the skin accompanied by a significant recruitment of macrophages, regardless of the infectious status of the flies (Fig. 1A and B). In order to visualize the bite site *in vivo*, an RFP-expressing strain of *L.m.* (*L.m.*-RFP) (14) (Fig. S1, A to D) and mice expressing eGFP under the control of the endogenous lysozyme M promoter (LYS-eGFP) (16) were employed. $eGFP^{hi}$ cells recovered from the skin of LYS-eGFP mice following *L.m.* infection are $CD11b^{hi}Gr\text{-}1^{hi}F4/80^{-}MHCII^{-}$ neutrophils while $eGFP^{lo}$ cells represent $CD11b^{+}F4/80^{+}MHCII^{+/-}Gr\text{-}1^{-}$ monocyte/macrophage populations (Fig. S1, E to G, see also Fig. S1, H to K and Fig. 4D). Two hours following exposure of the ventral ear pinnae of LYS-eGFP mice to either uninfected or *L.m.*-RFP-infected sand flies, GFP^{hi} neutrophils accumulated at sites of proboscis penetration through the skin (Fig. 1C).

2-photon intravital microscopy (2P-IVM) revealed that as early as 30” following exposure to sand flies, neutrophils had migrated into the skin and began localizing around apparent bite sites (Fig. 1D). Over the next hour, neutrophils rapidly accumulated in, and subsequently swarmed around, the vicinity of both infected and uninfected sand fly bites (Fig. 1D, and movies S1 and S2), eventually forming an epidermal “plug” through sequential migration of neutrophils into the hole left by the sand fly proboscis (Fig. 1E and S2, and movies S3 and S4). Parasite phagocytosis by neutrophils was readily observed during this recruitment process (movie S5) leading to the presence of large numbers of parasite-containing neutrophils at later time points (Fig. 1F and movie S6). In contrast to the rapid motility reported for mosquito-transmitted *Plasmodium* sporozoites, which appear to actively search for blood and lymphatic vessels (17,18), *L.m.* parasites appeared relatively immobile following sand fly delivery into the skin.

Due to the relatively low and variable number of parasites deposited by sand fly bite (14), intradermal (i.d.) needle inoculation of high numbers of infectious-stage *L.m.*-RFP metacyclic promastigotes was employed to quantitatively analyze the fate of parasites post-infection (p.i.). The pattern of neutrophil recruitment at early time points was similar to sand fly bite, although comparatively short-lived (Fig. S3). Two hours following injection of *L.m.*-RFP into the ear, analysis of all RFP^{+} dermal cells revealed that the vast majority of the *L.m.*-RFP signal was associated with the $CD11b^{hi}Gr\text{-}1^{hi}LYS\text{-}eGFP^{hi}$ neutrophil population (Fig. 2, A–D and S1N). These data are consistent with kinetic analyses of fixed tissue sections showing parasites initially interspersed between $F4/80^{+}GP^{lo}$ macrophages and subsequently phagocytosed by newly arriving $F4/80^{-}eGFP^{high}$ neutrophils (Fig. 2, E–F).

Dynamic analysis of neutrophil recruitment and parasite uptake revealed the rapid accumulation of neutrophils inside blood vessels surrounding the infection site as early as 30” p.i. and the subsequent diapedesis of these cells into the skin parenchyma (Fig. 2G and movie S7). Extravasating neutrophils were preferentially distributed to the side of the vessel facing parasite deposition and characterized by an extremely elongated uropod (Fig. 2H and movie S8). Neutrophils then moved in a highly directed manner towards the inoculation site (Fig. 2, G to I) where they rapidly and efficiently phagocytosed individual parasites (Fig. 2J). Phagocytosis occurred concurrently with migrational arrest, as demonstrated by a decrease in neutrophil mean velocity following parasite uptake (Fig. 2K). Additional data acquired following needle inoculation in the absence of parasites suggest that the initial inflammatory response to sand fly or needle-induced tissue damage drives the robust neutrophilic recruitment observed in these studies, overriding the potential contribution of any parasite-specific signals (Figure S4 and movie S9).

As macrophages are the definitive host cell for *Leishmania*, their relationship with neutrophils was explored. Mice expressing eGFP under the control of the endogenous MHC class II promoter (MHCII-eGFP) (19) (Fig. S1, L and M) were inoculated with *L.m.*-RFP. Phenotypic analysis of RFP-gated dermal cells at 18 hours p.i. revealed that the RFP signal was primarily associated with $CD11b^{hi}Gr\text{-}1^{hi}$MHC-II-$eGFP^{-}$ neutrophils and only small numbers of monocytes/macrophages or $CD11c^{+}$ DCs (Fig. 3A and S5). Strikingly, we observed an increase in the absolute number of RFP^{+} macrophages and a corresponding drop in the absolute number of RFP^{+} neutrophils over time (Fig. 3, C and D). By 6–7 days p.i the RFP signal was found primarily in the macrophage/monocyte population and only sparsely in neutrophils and $CD11c^{+}$ DCs (Fig. 3, B, D, and E). Although MHC-$II^{+}CD11c^{+}$ cells represented an extremely small proportion of infected cells at 1 day p.i., their increase in numbers by day 6 suggests that dermal DCs and/or Langerhans cells participate in the infectious process (20).

To determine the fate of *Leishmania* promastigotes following phagocytosis by neutrophils *in vivo*, infected and uninfected neutrophils were isolated from the ear dermis by cell sorting (Fig. 4, A to C). $GFP^{hi}RFP^{+}$ cells retained a normal cytoplasmic and nuclear appearance and contained intracellular *L.m.* parasites (Fig. 4, D) (21). Limiting dilution analysis of sorted neutrophils revealed that 92% of RFP^{+} but only 1.2% of RFP^{-} neutrophils contained at least one viable parasite (Fig. 4E). Furthermore, naïve mice inoculated with 10^3 $RFP^{+}GFP^{+}$ neutrophils or 10^3 cultured *L.m.*-RFP established equivalent infections (Fig. 4, F to H), demonstrating that *L.m.* phagocytosed by neutrophils are viable and can contribute to the establishment and progression of disease.

The extremely dense clusters of eGFP-expressing neutrophils and macrophages/monocytes that formed several hours following parasite inoculation (Fig. 3E) made visualization of individual cell-cell interactions difficult. To overcome this problem, sorted $GFP^{hi}RFP^{+}$ infected neutrophils were injected into the ears of transgenic animals expressing eGFP under the control of the macrophage/monocyte-specific CSF1 receptor promoter (22). Recipient animals were pre-exposed to sand flies 12 hours prior to neutrophil transfer in order to induce an inflammatory environment at the infection site. Utilizing 2P-IVM, we observed what appeared to be viable parasites (as indicated by their expression of RFP [Fig. S1, A to D]) being released from apoptotic neutrophils in the vicinity of surrounding macrophages (Fig. S6 and movies S10–S12).

We next examined the functional role of neutrophils on the establishment and progression of sand fly-transmitted Leishmaniasis. Mice treated with neutrophil-depleting antibody 16 hours prior to infected sand fly exposure had a specific and dramatic reduction of $CD11b^{+}$Ly-$6G^{+}F4/80^{-}$ neutrophils in the ear dermis 1 day after transmission (Fig. 4, I and J). In some, though not all experiments, reduced numbers of neutrophils were also observed in ears 6 days after transmission (Fig. 4J). Importantly, neutrophil depletion significantly reduced both the number of viable parasites detected per ear (Fig. 4L), as well as the incidence of ears with detectable parasites at 1 and 4 weeks post-transmission (Fig. 4M). Thus, the early influx and persistence of neutrophils following sand fly transmission of *L. m.* appears critical for the development of cutaneous disease.

The data presented here are relevant to the “Trojan Horse” model of *L.m.* infection (2) which postulates that uptake of infected neutrophils is a mechanism for ‘silent’ entry of parasites into macrophages. Our observations indicate that neutrophils are the initial host cell for a substantial fraction of parasites following infection and that neutrophil depletion results in reduced disease at 1 week p.i. We found no evidence, however, for uptake of intact, infected neutrophils by macrophages. In addition, macrophages were efficiently recruited to sites of infection and were able to directly phagocytose parasites in neutrophil-depleted animals

(Fig. S7). Under these conditions, macrophages and DCs did not acquire more parasites compared to non-depleted animals containing competing neutrophils, suggesting that neutrophils may facilitate infection by rescuing parasites not accessible to other phagocytic cells from death in extracellular spaces. Alternatively, infected neutrophils may release transitional stage parasites better adapted for macrophage uptake and survival, or macrophages may exhibit compromised microbicidal function in a setting in which they are heavily engaged in the anti-inflammatory process of clearing apoptotic neutrophils (23,24). This latter possibility is supported by an increase in the spontaneous release of the pro-inflammatory cytokines IL-1α and β by ear cells from neutrophil-depleted animals (Figure 4, N) (25).

The ability of phagocytic cells to rapidly localize to sites of tissue inflammation and subsequently capture and destroy pathogens is a hallmark of the innate immune response, highly conserved, and among the earliest observations in microbiology (26). We find that sand fly bites and needle inoculation induce an intense neutronphilic infiltrate into the skin, irrespective of parasite infection. These data are consistent with the finding that neutrophils are recruited to sites of sterile brain injury (27), and suggest that the predominance of *L.m.*-infected neutrophils at the site of parasite deposition is a byproduct of a host response aimed at wound repair and sterilization. Thus, the neutrophilic host response to the wound inflicted by arthropod vectors appears to have been a driving force in pathogen evolution aimed at counteracting and even exploiting the presence of these innate effector cells.

Supplementary Material

Refer to Web version on PubMed Central for supplementary material.

References

1. Peters N, Sacks D. Immunol Rev 2006;213:159. [PubMed: 16972903]
2. van Zandbergen G, Solbach W, Laskay T. Autoimmunity 2007;40:349. [PubMed: 17516227]
3. Segal AW. Annu Rev Immunol 2005;23:197. [PubMed: 15771570]
4. Nauseef WM. Immunol Rev 2007;219:88. [PubMed: 17850484]
5. Belkaid Y, et al. J Immunol 2000;165:969. [PubMed: 10878373]
6. Ribeiro-Gomes FL, Silva MT, Dosreis GA. Parasitology 2006;132 Suppl:S61. [PubMed: 17018166]
7. Charmoy M, et al. J Leukoc Biol 2007;82:288. [PubMed: 17449725]
8. Tacchini-Cottier F, et al. J Immunol 2000;165:2628. [PubMed: 10946291]
9. Chen L, et al. Parasitol Int 2005;54:109. [PubMed: 15866472]
10. van Zandbergen G, et al. J Immunol 2004;173:6521. [PubMed: 15557140]
11. Teixeira CR, et al. J Immunol 2005;175:8346. [PubMed: 16339576]
12. Kamhawi S, Belkaid Y, Modi G, Rowton E, Sacks D. Science 2000;290:1351. [PubMed: 11082061]
13. Belkaid Y, et al. Proc Natl Acad Sci U S A 2000;97:6704. [PubMed: 10841567]
14. Kimblin N, Peters N, Debrabant A, Secundino N, Egen J, Lawyer P, Fay MP, Kamhawi S, Sacks D. PNAS. In press.
15. Materials and methods are available at *Science* online.
16. Faust N, Varas F, Kelly LM, Heck S, Graf T. Blood 2000;96:719. [PubMed: 10887140]
17. Amino R, et al. Nat Med 2006;12:220. [PubMed: 16429144]
18. Vanderberg JP, Frevert U. International Journal for Parasitology 2004;34:991. [PubMed: 15313126]
19. Boes M, et al. Nature 2002;418:983. [PubMed: 12198548]
20. Soong L. J Immunol 2008;180:4355. [PubMed: 18354154]
21. Aga E, et al. J Immunol 2002;169:898. [PubMed: 12097394]

22. Burnett SH, et al. J Leukoc Biol 2004;75:612. [PubMed: 14726498]
23. Krysko DV, D'Herde K, Vandenabeele P. Apoptosis 2006;11:1709. [PubMed: 16951923]
24. Gregory CD, Devitt A. Immunology 2004;113:1. [PubMed: 15312130]
25. Matte C, Olivier M. The Journal of Infectious Diseases 2002;185:673. [PubMed: 11865425]
26. Martin P, Leibovich SJ. Trends in Cell Biology 2005;15:599. [PubMed: 16202600]
27. Kim JV, Dustin ML. J Immunol 2006;177:5269. [PubMed: 17015712]
28. We thank Kim Beacht for technical assistance, Hai Qi, Marc Bajénoff, Susanne Nylén, and Mary Ann McDowell for discussions, and Tom Moyer and Carol Henry for neutrophil sorting. GL113 and RB6-8C5 mAb were kindly provided by Antonio Rothfuchs (NIAID/NIH). This research was supported by the Intramural Research Program of the NIAID, NIH. The authors have no conflicting financial interests.

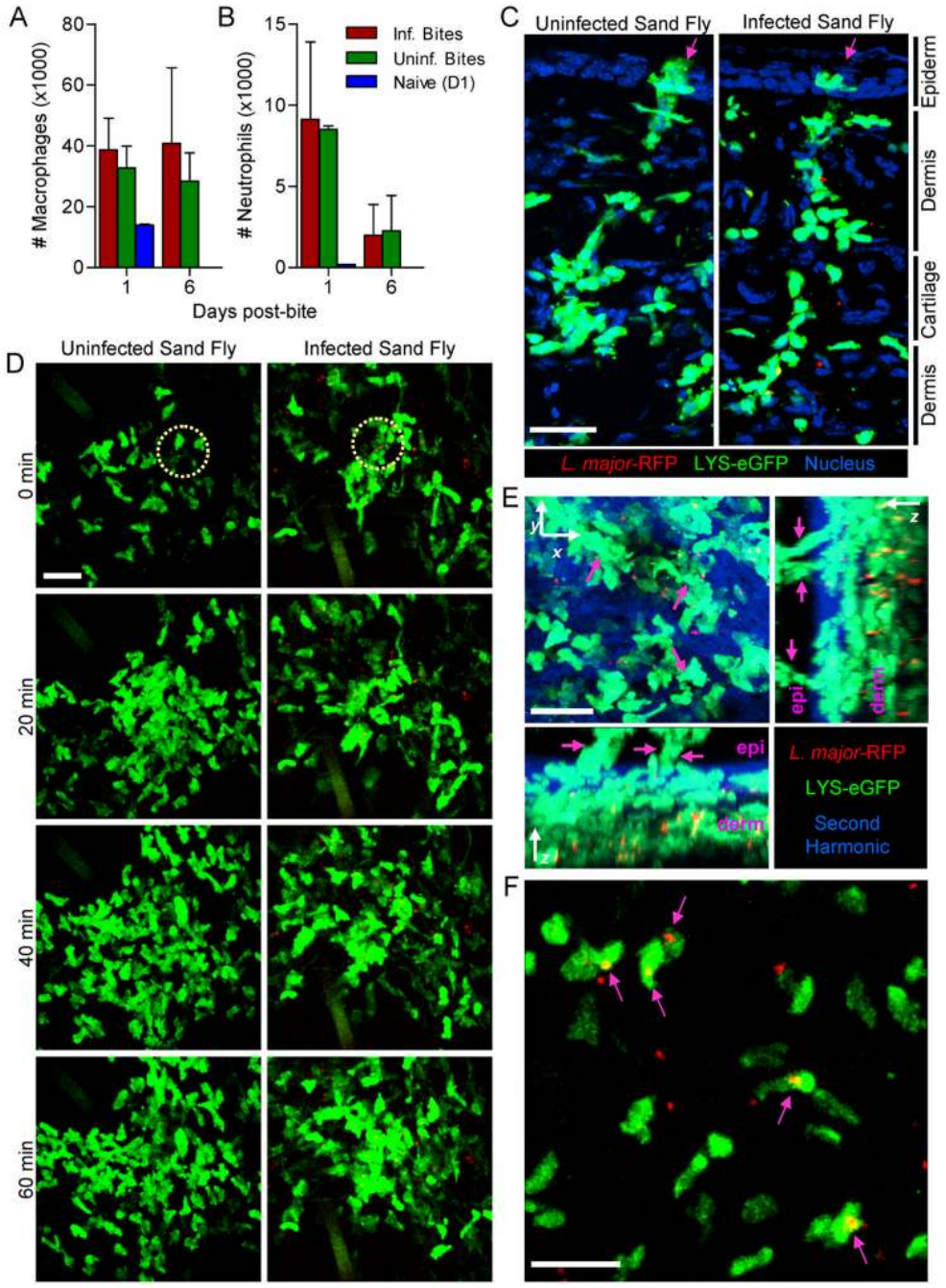

Figure 1. Neutrophils are rapidly recruited to sites of sand fly bite where they phagocytose *L. major* parasites

(A-B) Number of $CD11b^{+}F4/80^{+}$ macrophages/monocytes (A) and $CD11b^{+}Gr\text{-}1^{+}7/4^{+}F4/80^{-}MHCII^{-}Ly6G^{+}$ neutrophils (B) recruited into the ear (+/− SD; n≥4 ears/group/day) 1 or 6 days after being bitten by infected or uninfected sand flies. The number of cells in a naïve mouse ear is shown for day 1. **(C)** Ear sections from LYS-eGFP mice (green) bitten with uninfected (left) or *L.m.*-RFP (red) -infected (right) sand flies 2 hours prior to harvesting tissue. Arrows point to sites of proboscis penetration. See also movies S1 and S2. **(D)** 2P-IVM time-lapse images from the ears of LYS-eGFP mice (green) beginning 40” after exposure to uninfected (left) or *L.m.*-RFP (red) -infected (right) sand

files. Circles represent sites of sand fly proboscis penetration. **(E)** Maximum intensity projection images across X, Y, and Z dimensions derived from 2P-IVM of the ear of a LYS-eGFP mouse (green) 2 hours after exposure to *L.m.*-RFP (red) -infected sand flies. Dermal and epidermal layers defined by the presence or absence of collagen (blue), respectively, are indicated. Arrows point to sites of proboscis penetration and neutrophil "plug" formation. See also movies S3 and S4. **(F)** Image obtained from a 2P-IVM time-lapse series of the ear of a LYS-eGFP mouse (green) 3 hours after exposure to *L.m.*-RFP (red) -infected sand flies. Arrows point to neutrophils with one or more intracellular parasites. See also movies S5 and S6. Scale bars, 30μm (C–E), 20μm (F).

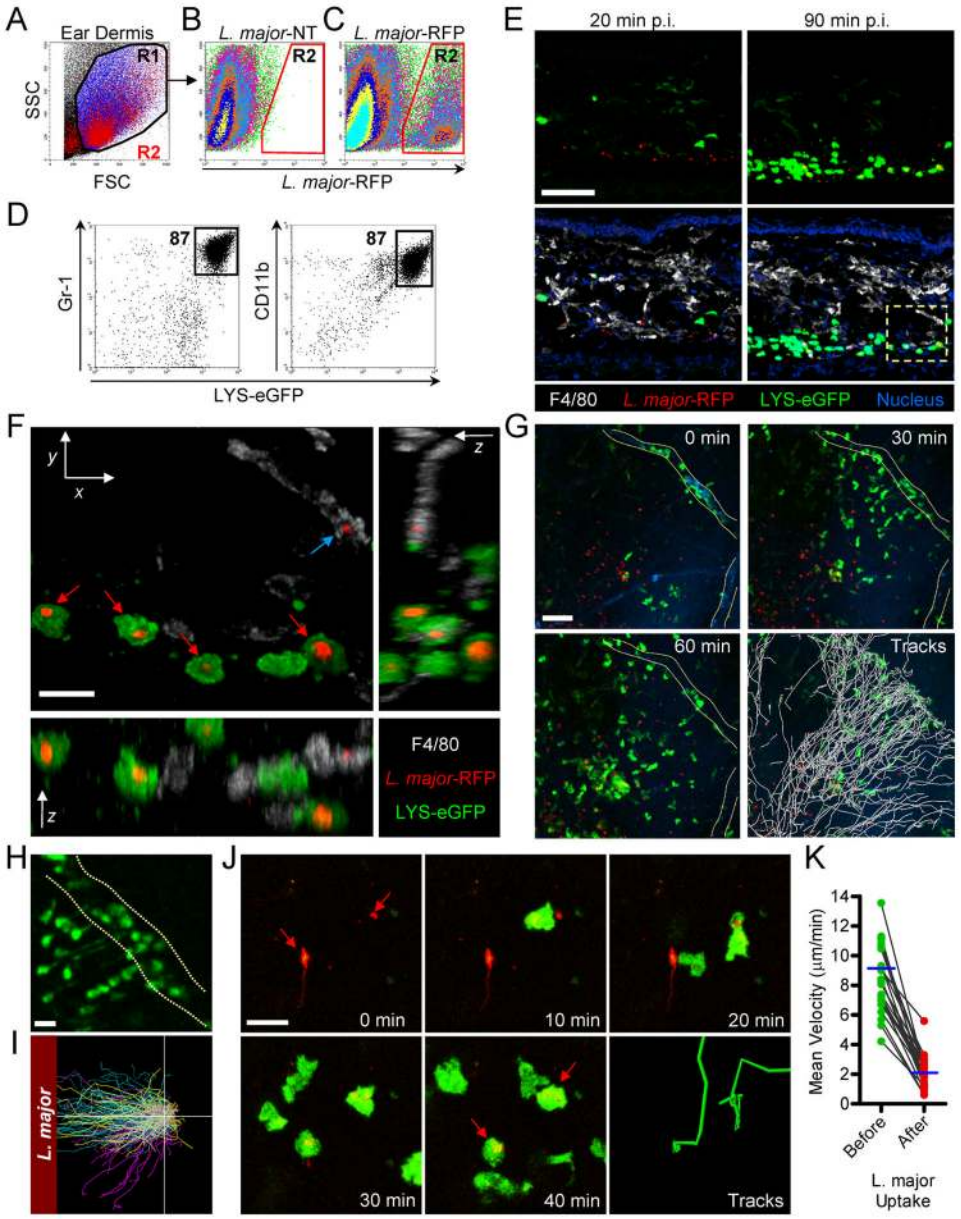

Figure 2. Rapid recruitment and infection of neutrophils following intradermal inoculation of *L. major*

(A) SSC/FSC dot plot of ear-derived cells 16 hours p.i. with 10^6 *L.m.*-RFP. **(B and C)** SSC/RFP dot plots of R1 gated ear cells 16 hours p.i. with 10^6 *L.m.*-empty vector control (B) or *L.m.*-RFP (C). **(D)** GFP, Gr-1, and CD11b expression by RFP^+ R2 gated cells from ears of LYS-eGFP mice 2 hours p.i. with 5×10^5 *L.m.*-RFP. **(E)** Ear sections from LYS-eGFP mice 20" (left) or 90" (right) p.i. with 1×10^4 *L.m.*-RFP stained with F4/80 (white) and a nuclear dye (blue). Top panels show GFP and RFP images while bottom panels show a merge of all channels. **(F)** Maximum intensity projection images across X, Y, and Z dimensions from boxed region in part E. Red arrows indicate *L.m.*-RFP phagocytosed by neutrophils and blue arrow indicates a parasite captured by a macrophage.. **(G–K)** LYS-eGFP animals were subject to 2P-IVM 30" p.i. with 1×10^4 *L.m.*-RFP. (G) Time-lapse images showing GFP^+ (green) cells, *L.m.*-RFP (red), and blood vessels (blue). Bottom right panel labeled "Tracks"

shows the paths followed by cells from the vessel to site of inoculation of parasites over 60". (H) Magnified view from part G showing neutrophil extravasation from vasculature. See also movies S7 and S8. (I) Cell migration paths from three independent experiments (cyan, yellow, and purple tracks) were normalized for their origin and their position relative to the site of parasite deposition. (J) Time-lapse images showing neutrophil (green) migration before and after phagocytosis of *L.m.*-RFP (red, arrows). (K) Neutrophil mean velocity 10" before and 10" after parasite phagocytosis. Data points represent individual cells and were compiled from 4 separate experiments. Scale bars, 50μm (E,G), 15μm (F,H,J).

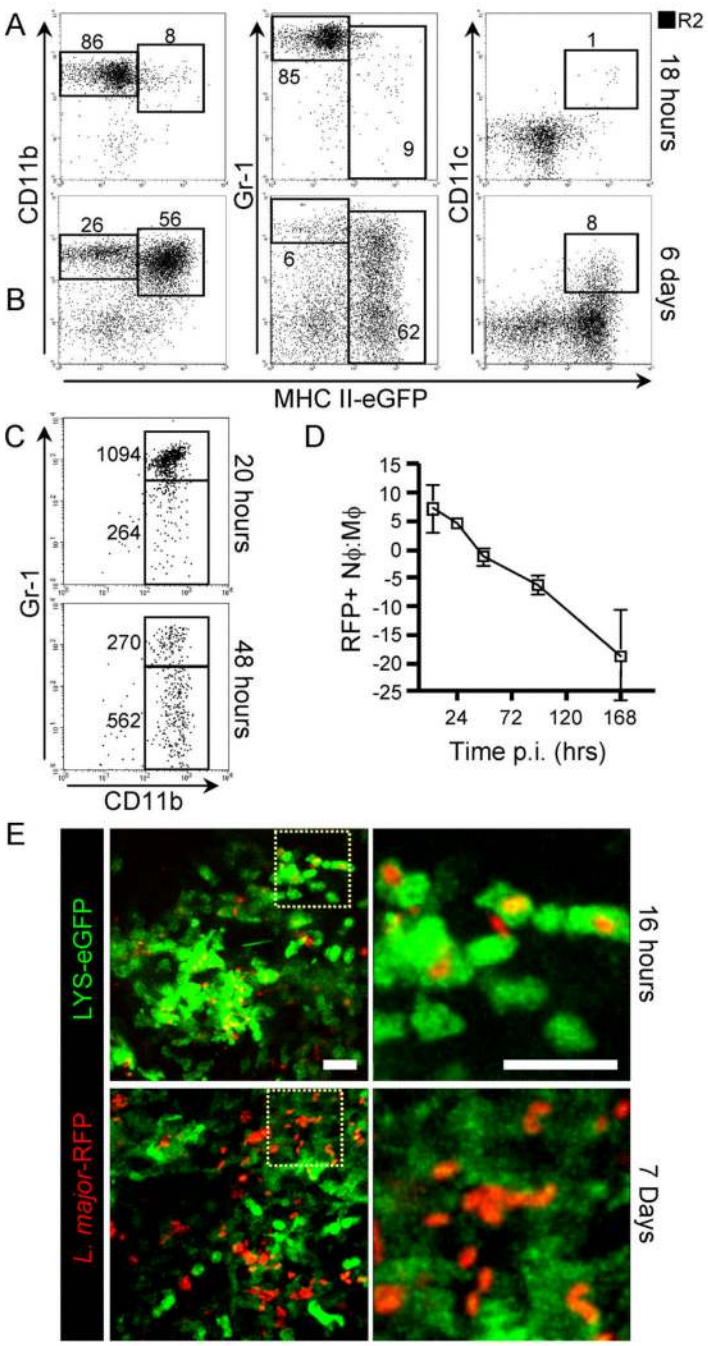

Figure 3. *L. major* transitions from neutrophils to macrophages early after intradermal inoculation

(A-B) Dot plots gated on RFP$^+$ cells (R2 in Fig. 2C) from ears of MHC II-eGFP mice taken at 18 hours (A) or 6 days (B) p.i. with 1×10^6 *L.m.*-RFP. **(C)** CD11b and Gr-1 expression of RFP$^+$-gated cells at 20 and 48 hours p.i. Numbers indicate the absolute number of gated cells per sample. **(D)** Mean of the ratio +/− SD of RFP$^+$ infected neutrophils to RFP$^+$ infected macrophages/ monocytes, n=4–6 individual ears per time point. **(E)** 2P-IVM projection images from the ears of LYS-eGFP mice (green) at 16 hours or 7 days p.i with 1×10^4 *L.m.*-RFP (red). Images on right are magnified views of the boxed regions. Scale bars, 20μm.

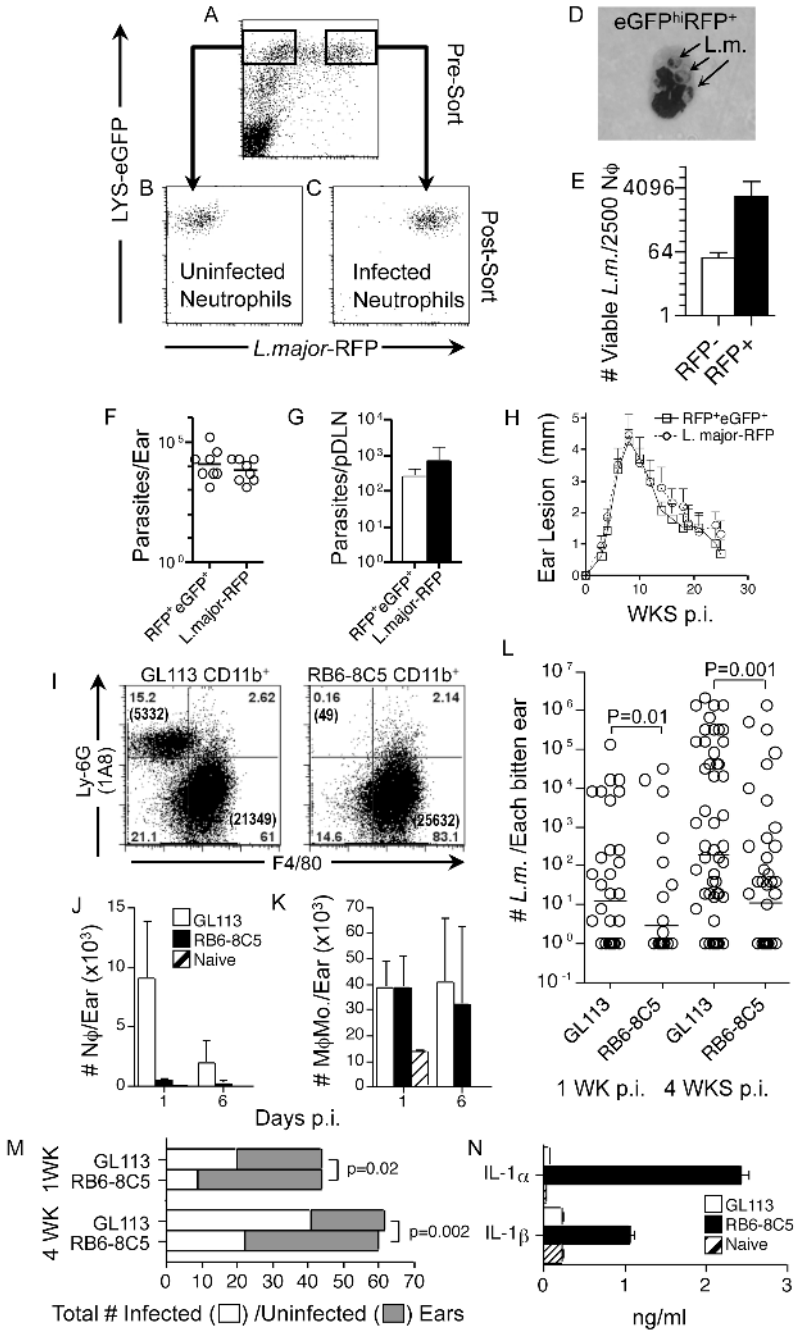

Figure 4. Neutrophils harbour viable parasites and promote productive infections

(A-D) LYS-eGFP^{hi} neutrophils from the ear 12 hours p.i. with 2.5×10^6 *L.m.*-RFP were sorted into uninfected RFP$^-$ (B) or *L.m.* infected RFP$^+$ (C and D) populations. (B and C) Post-sort. (D) Dif-Quick stain of the cytospun GFP$^+$RFP$^+$ post-sort population. **(E)** Number of viable parasites per 2500 RFP$^-$ and RFP$^+$ neutrophils (+/− SD of triplicate samples). **(F–H)** Wt mice were injected in the ear with 10^3 culture-derived *L.m.*-RFP metacyclic promastigotes or 10^3 RFP$^+$GFP^{hi} infected neutrophils. Twenty-one days following injection mice were assessed for parasite load in individual ears (F), in pooled DLNs (G), and mean +/− SEM (n=8) ear lesion diameter over the course of infection (H). **(I–N)** Mice were treated with control (GL113) or neutrophil depleting antibody (RB6-8C5) 16 hours before

exposure to infected sand flies. (I) Representative dot plot of $CD11b^+$ gated $Ly\text{-}6G^+F4/80^-$ neutrophils and $Ly6G^-F4/80^+$ macrophages/monocytes on day 1 p.i. Analysis of the total number of $CD11b^+7/4^+F4/80^-MHCII^-Ly6G^+$ neutrophils (J) and $CD11b^+F4/80^+$ macrophage/monocytes (K), per ear +/− SD (n≥4/group/day), on day 1 and day 6 p.i. (L) Parasite loads in individual ears at 1 and 4 weeks following exposure to infected sand flies in GL113 versus RB6-8C5-treated animals as determined by limiting dilution analysis. Each open circle represents a single exposed ear in 3 (WK1) or 4 (WK4) pooled experiments. (M) Representation of the total incidence of infected versus uninfected ears in RB6-8C5 versus GL113 treated animals at 1 week (odds ratio =0.299, 95% CI (0.097, 0.847), p=0.020) and 4 weeks (odds ratio =0.293, 95% CI (0.126, 0.658), p=0.0017) post transmission as determined by limiting dilution analysis. **(N)** Spontaneous release of IL-α and β by ear derived cells as determined by multiplex cytokine analysis at 1 week p.i.